4 Photomultipliers

4.1 Introduction

The width of the instrument response function in the single photon counting experiment is due to a combination of three principal factors, namely, the duration of the excitation pulse, the spread in transit time of photoelectrons in the fluorescence photomultiplier tube and timing jitter in the electronic components. The fluorescence photomultiplier (PM) is therefore a crucial component of the apparatus and in this chapter we deal briefly with its operation.

As was stated in Chapter 2, the PM serves merely to time individual photons emitted by the sample, and does not produce an analogue representation of the decay of emission. Consequently many of the dark noise problems associated with current pulse operation of PMs are avoided. Since the PM is exposed only to a very low level of radiation occurring in well separated pulses, photomultiplier fatigue (Lopez and Rebolledo, 1981) is not important in SPC measurements (Coates and Andrews, 1981). In addition the rise time of the PM anode pulse is in itself unimportant since the discriminator merely times the arrival of this pulse. What is important in the measurement is not, strictly speaking, the transit time spread of photoelectrons, but the statistical dispersion associated with this spread. That is, time resolution is dependent on the uncertainty in the delay time between the emission of a photoelectron from the cathode and the arrival of the corresponding electron pulse at the anode (Birks and Munro, 1967). As the transit time and corresponding spread become shorter the dispersion decreases and time resolution increases. It must be remembered, however, that the time resolution in the SPC technique is not equal to the total instrumental time uncertainty. The technique achieves its superior time resolution because it is a statistical technique deriving its results from a very large number of independent experiments (individual excitation pulses).

It is not intended in the following sections to give a technical description of the mechanisms governing photoelectron ejection and secondary emission. Rather we concentrate on pointing out the aspects of the PM operation that affect the time-correlated SPC experiment. Brief details are also tabulated concerning some commonly used PM tubes. It should be noted, however, that not all photomultipliers are suitable for timing operation and the

prospective purchaser should verify with the manufacturer that the PM he wishes to purchase will suit his needs. Incidentally, the early drawbacks in this regard associated with group III–IV elements as photocathode materials (Longworth, 1977) seem to have been overcome. A more complete account of single photon photomultiplier detection has been given by, for example, Poultney (1972). Much useful information can also be found in the Application Manuals published by the manufacturers whose addresses are listed in Appendix 4.A2. For details related to the possible incorporation of a PM tube on the trigger channel of the instrument the reader is referred to Section 3.

Fast PM tubes which are suitable for single photon detection can be classified into four main groups:

(1) Side-on tubes with Venetian blind dynode structure. These tubes usually have a small number of multiplication stages (e.g. 9) and consequently a low gain. They are by far the least expensive of the four types.
(2) End-on tubes with linear focussed dynode structure, a large number of stages (e.g., 12 or 14) and a high gain. They are quite expensive, particularly when specially selected for low dark noise. This type of PM is standard in SPC instruments.
(3) Crossed-field photomultipliers, the electron focussing in which is achieved by means of crossed electric and magnetic fields. These tubes have very fast rise times and are reported to be free of the after-pulsing commonly observed in the electrostatically focussed tubes listed in (1) and (2). They have a low gain however and are quite expensive.
(4) Channel photomultipliers in which a continuous secondary emission coating within a cylindrical microchannel carries out the multiplication (Timothy and Bybee, 1977). Again these devices have a low gain and are quite expensive. They have, however, extremely fast rise times and seem likely to supplant conventional PM tubes as detectors in picosecond single photon counting instruments.

To date the most common PM tubes in SPC experiments have probably been the Philips (Amperex) 56DUVP/03 and the RCA 8850. Both of these tubes have given very satisfactory performance but are now being superseded by faster devices. They are not particularly suited for detection of long wavelength (>650 nm) emission, for which purpose red-sensitive equivalents are available. For detection of vacuum u.v. radiation solar-blind PM tubes with appropriate window materials, available for example from the EMR company*, have proved satisfactory. Readers who may wish to detect radiation of even higher energy are referred to the discussion of windowless

*EMR Photoelectric (see Appendix 4.A2).

PM tubes in the book by Samson (1967). In recent years inexpensive side-on tubes have gained in popularity; in one commercial SPC instrument* this type of tube is standard. With the increasing proliferation of mode-locked lasers as excitation sources, however, there will be a corresponding demand for PM tubes with time resolution of the order of picoseconds. Microchannel plates, while suffering from the serious disadvantage of low gain, appear now to offer a time resolution increased by a factor of 5 or 10 over the other varieties of PM. In the following sections we shall outline some of the important properties of the single photon detector with reference to specific PM tubes, the performance of which has been described in the SPC literature. Some of the photomultipliers and their characteristics are listed in Appendix 4.A1.

4.2 Characteristics

4.2.1 Spectral response

The spectral sensitivity of the PM depends on the cathode material and in a somewhat trivial sense, on the window material. Quartz or sapphire windows are necessary for radiation from 300 nm to 180 nm (the cut-off of fused silica) and are thought to be less fluorescent than pyrex windows. There are a large number of cathode materials, the responses of which can be seen in the manufacturers' catalogues. The standard bialkali (KCsSb) response is from 250 to about 650 nm. Red sensitive PMs, suitable for single photon counting, are available from most PM tube manufacturers and extend this wavelength range to 850–900 nm.

Of this type the RCA C31034 has attained some popularity (Spears and Hoffland, 1977) and the inexpensive side-on type, Hamamatsu R928 has also been reported as satisfactory (Kinoshita *et al.*, 1981). It will usually be necessary to cool the red-sensitive photocathode in order to reduce excessive thermionic emission (see Section 4.2.3) although the red-sensitive EMI 9863 QB has an acceptably low level of dark noise at room temperature (Lampert, 1981). Work in the vacuum u.v. as far as 110 nm can be accomplished with PM tubes having MgF_2 or LiF windows. For instance Lyke and Ware (1977) described the performance of an EMR 561F-09-13 tube with an MgF_2 window in this wavelength region. Dark current in such solar-blind tubes is extremely low, an advantage offset to some extent by low gain arising from low photocathode quantum efficiency.

*Photochemical Research Associates (see Appendix 3.A1).

4.2.2 Gain

Detected light levels in single photon counting are very weak; as a consequence it has been traditional to detect single photons with high gain PM tubes. Since high gain is generally achieved by increasing the number of multiplication stages (dynodes) the price paid has usually been a decrease in time resolution. For instance it will be seen in Appendix 4.A1 that the Philips 56DUVP/03 (Lewis *et al.*, 1973), which has 14 stages, achieves a gain of 2×10^8 (the highest quoted gain, incidentally, of all SPC PM tubes known to us) with a photoelectron transit time of 43 ns. The manufacturer, wishing to develop an equivalent of this tube with a shorter transit time reduced the number of stages to 12 in the XP2020 (Lampert *et al.*, 1983) thus reducing the transit time to 28 ns but at the same time decreasing the gain by almost a factor of 10.

Low gain can be compensated for by amplifying the PM anode pulses before discrimination, by discriminating at a low amplitude level or by operating the photocathode at a higher potential relative to the anode. As a consequence there is a steadily increasing tendency to employ PM tubes with a small number of dynode stages such as the red-sensitive RCAC31034, an end-on type with 11 stages, or the side-on 9 stage types, e.g., RCA1P28 and Hamamatsu R928. The latter has a surprisingly high gain but has a response that seems to depend strongly on the area of the photocathode illuminated (see Section 4.2.4).

Gains specified in the manufacturers' data sheets can usually be improved upon by operation of the photocathode at a higher relative potential than the common operating potential. Tube performance, especially as regards dark current, may degrade more rapidly if the manufacturer's maximum rated voltage is exceeded, but it is likely that this rating is conservative in most cases. We have operated an RCA 1P28 at 1500 V (the manufacturer's maximum rating is 1250 V) for a number of months without any apparent degradation in performance. (Actual arcing between dynodes does not occur in this tube until the interstage potential reaches 460 V (Beck, 1976).) Damage to inexpensive tubes of course is not serious; it would be perhaps more prudent not to exceed the maximum rating for the expensive types.

Owing to fluctuations in the multiplication process the total charge developed is subject to a statistical uncertainty (Jones *et al.*, 1971; Wright, 1981). As a result the anode pulses generated usually show large variations in pulse height, which require complicated discriminator circuitry for correct timing (see Section 5.2.2). This feature is less pronounced in side-on tubes when operated at a high voltage (Kinoshita *et al.*, 1981).

Discrimination of PM anode pulses with levels as low as 5 mV can be accomplished with many, but not all, constant fraction timing discriminators.

A low discriminator level is advantageous from the point of view of acceptance of relatively more single photon pulses (see Section 5.3), but may result in a somewhat inferior signal-to-noise ratio and increased interference from spurious r.f. signals. If this source of distortion is absent and the PM tube is not too noisy, low gain may be satisfactorily tolerated without having recourse to an amplifier or preamplifier. These, however, are in common use and may in fact lead to improved performance. With microchannel plate PMs in particular, e.g., the Hamamatsu R1294U-01, which have extremely low gains but extremely rapid transit times, amplification of the anode pulses will probably be necessary. Marconi Inc., Hewlett Packard Inc. and Ortec Inc. (see Appendix 5.A1) market amplifiers and preamplifiers that are reported to give satisfactory performance.

4.2.3 Dark current

A high dark current is not usually a critical problem in single photon counting experiments, both because the background is easily subtracted from the observed data and also because dark counts occurring outside the TAC range are ignored. Nevertheless it is desirable to maintain the dark counts as low as possible, especially if weakly fluorescing samples are under investigation or if the emission is longlived. Dark count levels, even among PM tubes of the same type, seem to vary enormously from one tube to the next. Consequently it has been customary to have the manufacturer select from his stock, at an extra cost, a tube with low dark count level. While the extra outlay is probably justified the tube so selected should be checked before final purchase, since the selection might be based on a count rate obtained at a low operating voltage.

Dark current can be permanently increased if high levels of light are allowed to impinge on the PM tube, when polarized. Even when unpolarized it should not be exposed to room light for long (>1 min) periods. Initial dark count rates can be substantially reduced through polarization of the tube with no incident light; in fact it is customary, in instruments that are always shielded from room light and when safety is not at risk, to leave the high voltage permanently on. It is common practice to operate the PM with the photocathode at a negative potential with respect to earth and the anode at earth potential. Operation with the anode at high positive potential and the cathode earthed reduces the number of noise pulses, presumably by suppressing electroluminescence from the glass envelope which is maintained at cathode potential (Leskovar *et al.*, 1976). An unacceptable dark current level cannot be definitely specified. A rough guide to performance however is our observation that, at a discriminator level of about 70 mV, common tubes

have a dark rate of certainly less than 500 Hz and more usually in the range 50–250 Hz. This is not to say that if the dark count exceeds this level the tube should be rejected. It should also be remembered that water vapour round the PM pins and condensed on the tube envelope increases the noise. In humid conditions, therefore, it is advisable to keep the PM housing continually flushed with dry nitrogen. Operation with the cathode at earth potential is reported to be particularly effective for noise reduction in a humid atmosphere (Halpern, 1974).

Undoubtedly the most effective means by which dark counts can be reduced is by cooling the photocathode. As we stated previously, red-sensitive photocathode materials generally have an intolerably high level of thermionic emission at room temperature, and many red-sensitive PMs must be cooled. Usually bialkali photocathodes (e.g. KCsSb) show no decrease in dark count when cooled below $-10°C$ and should not in any case be cooled below $-30°C$. On the other hand, red-sensitive photocathode materials such as AgOCs (S1 response) and trialkali (S20), may be cooled to $-180°C$ and in general show increased dark counts above $-30°C$.

Conveniently compact thermoelectrically cooled PM housings are available commercially* for both side-on and end-on tubes. Alternatively a cooled liquid can be circulated through coils wound round the housing. If the cathode is operated at a negative potential with respect to earth the tube envelope is at the same potential, and coils cannot be allowed to touch it. When the tube and housing are cooled below 0°C care must be taken to ensure that water vapour condensed on windows and dynode pins does not limit intensity or increase the dark count rate. Dry nitrogen flushed continuously through the housing (if the PM chamber is not sealed) and passed over the housing window should eliminate any condensation.

4.2.4 Transit time

An electron ejected from the cathode causes the transmission of an electron bunch along the dynode chain of the photomultiplier. The transit time is the elapsed time between the moment of ejection of the cathode photoelectron and the arrival of the corresponding electron bunch at the anode. Since electrons ejected in the multiplication process will have a range of velocities and may also travel along different paths there will be a spread in transit times of the order, in a conventional PM, of 1 or 2 ns. In the 12-stage RCA 8850, Leskovar *et al.* (1976) report a transit time spread of 0.41 ns. Transit time spreads are not listed in Appendix 4.A1 because of lack of data. The

*From Products for Research (see Appendix 4.A2).

available data indicate that the spread is roughly proportional to the transit time and in very many cases equal to the anode pulse rise time (Lytle, 1974). Consequently a reduced transit time yields a reduced transit time spread and, by implication, a reduced statistical dispersion (see Section 4.1) with an ensuing increase in the time resolution of the experiment.

The spread in transit times depends on, amongst other things, the energy of the primary photoelectron, the point on the surface from which it is emitted, and the extent to which the resulting time spread can be minimized by electrostatic focussing. An estimate of transit time spread can be determined with the assumption that the dynodes are parallel plates distance d apart (Beck, 1976). If the p.d. between them is V volts an electron will travel a distance d in a time t given by

$$t = d\left(\frac{2m}{eV}\right)^{1/2}, \tag{4.1}$$

where m and e are the mass and charge of the electron, respectively. The decrease in transit time for an electron starting with an energy V_0 is roughly

$$\Delta t \approx \left(\frac{V_0}{V}\right)^{1/2} t \tag{4.2}$$

$$\approx \left(\frac{d}{V}\right)\left[\left(V_0 \frac{2m}{e}\right)\right]^{1/2}. \tag{4.3}$$

Similarly the transit time spread per stage resulting from a path difference Δd is roughly

$$\Delta t = \Delta d\left(\frac{2m}{eV}\right)^{1/2}. \tag{4.4}$$

In fact transit time spreads determined from these equations are too high. Nevertheless the inverse dependence on interdynode potential is clear. Wavelength dependence in transit time spreads will be considered in Section 4.4 and dynode chain voltage dividers in Section 4.3.

Present day end-on PM tubes and their dynode chains are designed so as to minimize the time difference of travel from different points on the photocathode to the first dynode. A focus or grid electrode is incorporated for this purpose. It is nevertheless observed that the shape of the measured decay curve and the position of its maximum vary with the area of the cathode illuminated, especially if the voltage divider network is improperly adjusted (Lewis *et al.*, 1973; Leskovar *et al.*, 1976). Unless the scattered photons for the instrument response function measurement and the fluorescence photons strike the same area of the photocathode difficulties in deconvolution will ensue. In order to reduce the effects of this artefact the

fluorescence and scatter should, if possible, emanate from the same volume (see Section 2.2.4). It also helps to mask the PM windows with a black screen with a small hole in the centre. The screen, which will undoubtedly also reduce the count rate, should be positioned as close as possible to the window without touching it.

Side-on PM tubes, which were not originally designed for timing purposes, are more prone to transit time variations resulting from path length difference between the cathode and first dynode than end-on tubes. Since there are no focussing electrodes these path differences, the possibilities for which can be clearly seen in the diagram of Fig. 4.1, are not equalized. Figure 4.1 applies to PM tubes like the RCA 1P28 with a viewing window that can be as much as 3.5 cm long by 1 cm broad. The effect of illumination of different points on this surface on the transit time spread is shown in Fig. 4.2, which is adapted from the work of Kinoshita *et al.* (1981). It can be seen that the principal effect of varying transit time spread is a shift in the position of the instrument response function, although a change in shape also occurs. It is important therefore to illuminate the same area of the photocathode throughout the SPC experiment. Since transit time spread also depends to some extent on the operating voltage as indicated by Equations 4.3 and 4.4, it is customary to operate SPC PM tubes at the maximum voltage recommended by the manufacturer.

4.2.5 Single photon resolution

In some PM tubes designed for timing applications, anode pulses corresponding to single photon events have a voltage distribution that is easily distinguishable from pulses corresponding to two and three photon events. This single photon pulse height resolution (Foord *et al.*, 1969) is very well defined in two commonly used RCA PM tubes, namely the 8850 (Morton *et al.*, 1968) and the C31034 (Gulari and Chu, 1977). The pulse height

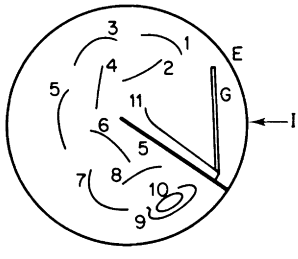

Figure 4.1 Dynode configuration of common side-on type PM tube (top view). 1–9, dynode numbers; 10, anode; 11, photocathode; G, grill; I, incident light; S, screen; E, glass or quartz envelope.

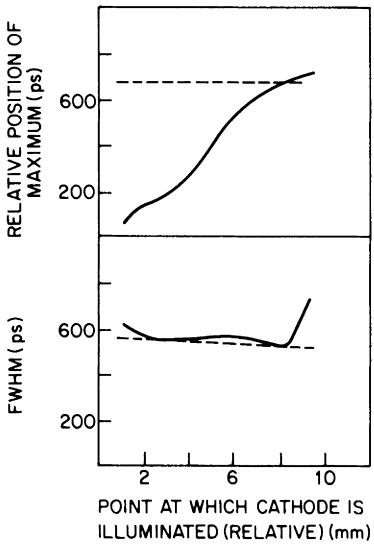

Figure 4.2 Variations of position and FWHM of instrument response function with point of illumination of side-on PM photocathode along short side (——) and long side (- - - - -) (after Kinoshita *et al.*, 1982).

spectrum of the RCA 8850 PM is illustrated in Fig. 4.3. Single photoelectron distributions for some EMI tubes have also been measured (Wright, 1981). The pulse height spectrum for the PM tube is obtained as follows (Morton, 1968; Kouyama, 1978). A low level of light is allowed to impinge on the photocathode. The signal from the anode or one of the later dynodes is routed to an integrating preamplifier, which essentially sums the amplitudes of all pulses input during a fixed time interval (say 50 μs) and outputs a pulse the amplitude of which is proportional to this sum. (The Ortec 113

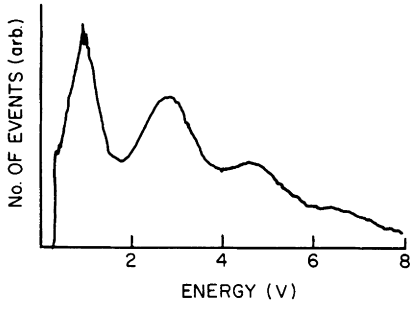

Figure 4.3 Pulse height spectrum for RCA 8850 PM tube operated at 2400 V (after Schuyler and Isenberg, 1971).

preamplifier is the usual choice.) It is generally necessary to amplify the PM pulses by a factor of *c.* 1000; therefore the pulses from the preamplifier may have to be routed to a second amplifier. However, the multichannel analyser, in which the spectrum is recorded, may possess sufficient amplification. The signals are routed to the AMP input of the MCA (see Section 5.2.7) and counts are accumulated in pulse height analysis mode. Channels now represent increments in energy so that the accumulated counts will show peaks corresponding to one-, two-, three- etc., photon events. If the level of light striking the photocathode is increased the peaks corresponding to more than one photon should grow in intensity (Kouyama, 1978). If necessary, the analyser channels may be calibrated with signals of known energy (Foord *et al.*, 1969).

On the basis of the pulse height spectrum a pile-up inspector may be designed, but only if the spectrum has a fairly narrow peak corresponding to single photoelectron events. For this purpose the signal to be inspected is taken from the last dynode, since the anode pulse is routed to the TAC. Therefore for the spectrum on which the energy window in the single channel analyser is based (see Section 5.2.5(b)), signals from this dynode should be processed. Pile-up inspection can reduce data collection times and may be advisable if thermally or photochemically unstable materials are under investigation. It depends for its success, however, on a small overlap between the energy distributions for one- and two-photoelectron events. Kouyama (1978) resolved the spectrum for the RCA 8850 into distinct distributions corresponding to one photon, two-photon and three-photon events, and showed that a suitable energy window can be chosen for the output pulses of this tube. In Section 5.2.5(b) the disadvantages attending pile-up inspection are discussed.

4.2.6 Magnetic focussing and screening

Transit time fluctuations can be reduced by focussing the electron bunch with a magnetic field. Magnetic focussing in conventional PM tubes, however, may create fringe areas in the photocathode and cause after-pulsing (Coates, 1975). Consequently it is rarely employed as a means of improving the timing capabilities in SPC experiments of conventional PM tubes. On the other hand, the recently-developed crossed-field photomultiplier, which employs crossed electric and magnetic fields for focussing purposes, is now commercially available and is suitable for single photon counting (see Section 4.5).

Accidental magnetic fields may interfere with the electron focussing and increase dark counts. It is therefore common to screen the PM tube from external magnetic fields by surrounding the tube with a cylinder of so-called mu-metal. Cylinders of this type, available from most PM tube manu-

facturers, should be about 1 cm longer than the length of the PM tube as illustrated in Fig. 4.4. The cylinder of mu-metal is preferably maintained at cathode potential and if the latter is at negative high voltage the cathode pin is attached through a high resistor (e.g., 6 MΩ) to the mu-metal. This connection should be made without subjecting the metal to undue strain, which might degrade its magnetic properties. Since the screen is now at high negative potential it must be insulated from the housing. A simple unscaled design for a housing, including magnetic screen, for an end-on PM tube is illustrated in Fig. 4.4.

4.2.7 Anomalous pulses

A cursory glance through the SPC literature will reveal that instrument response functions measured in most laboratories contain a secondary peak or shoulder that is thought not to be present in the pump pulse profile. It is now generally believed that this peak is a result of some photomultiplier process and it is usually displaced from the main peak by a fixed amount that depends on the particular PM tube. It seems, however, that this secondary peak is not present in instrument response functions measured with side-on PM tubes. A peak preceding the main peak is also sometimes observed.

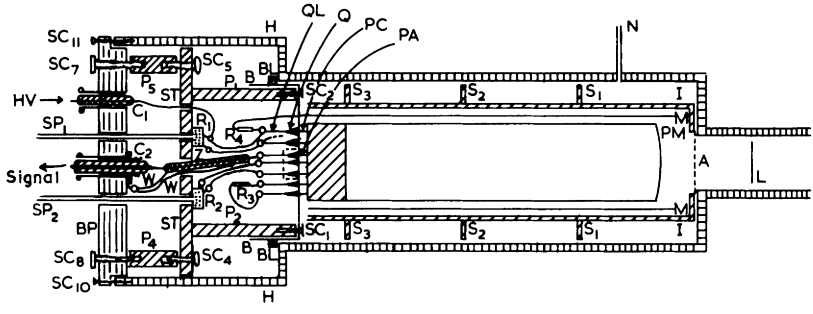

Figure 4.4 Design of housing for end-on PM tube (not drawn to scale) H, aluminium housing; N, port for N_2 flushing; L, lens or iris or quartz plate; A, aperture (if desired); I, plastic insulating cylinder; S_1–S_3, plastic lips on insulating cylinder; M, cylinder of mu-metal; B, commercial base with pin sockets (Q); QL, socket lugs; BL, lip on base; PC, cathode pin; PA, anode pin; R_4, resistor between mu-metal and cathode (*c.* 6 MΩ); R_3, fixed resistance; R_1,R_2, variable resistors (rheostats) mounted on stage (ST) with spindles SP_1, SP_2, ... protruding through back plate (BP); P_1,P_2(P_3 not shown), plastic posts connecting stage to base and attached with plastic (nylon) screws, SC_1,SC_2(SC_3); Z, coaxial cable; W, braid in coaxial cable; P_4,P_5(P_6 not shown), plastic posts attaching stage to back plate and connected with screws SC_4, SC_5(SC_6), SC_7, SC_8(SC_9); BP, back plate stepped so that r.f. seal (solder gasket) may be inserted; C_1, high voltage bulkhead plug; C_2, BNC type bulkhead plug.

The mechanisms that give rise to these spurious peaks are not known with certainty. After-pulsing is thought to occur as a result of an internal electron reflection, possibly from the first dynode to the photocathode (Stevens and Longworth, 1972). Whether a reflection over so short a length could cause (for the RCA 8850) a peak shifted by as much as 22 ns (Schuyler and Isenberg, 1971) is open to question. Whatever the cause, this peak can be minimized by careful adjustment of the interdynode voltages (see Section 4.3) and seems not to affect the success of deconvolution provided that it can be reduced to less than 1% of the height of the main peak. It should be borne in mind that flash lamps and pulsed lasers may produce real optical peaks which should not be confused with a peak resulting from a PM artefact (see Section 3.3). Unlike the peak resulting from after-pulsing, the early-time spurious peak seems to interfere seriously with successful deconvolution. It has been surmised that this peak results from photons that are not absorbed by the cathode but eject a photoelectron from the first dynode (Hartig *et al.*, 1976). It can be eliminated entirely through correct choice of interstage voltages. While a slight shoulder on the rising edge of the instrument response function will probably be tolerable in deconvolution, the intensity in this peak should be reduced as much as possible. In theory anomalous peaks should not affect mathematical analysis if they are produced in the same way in the measurements of instrument response function and decay curve. That they do implies perhaps that the mechanisms by which they are produced are influenced by some factor that changes between the two measurements, possibly the area of the cathode illuminated or the angle of illumination. Voltage divider adjustments might then be minimizing the effect of this factor on transit time spread while at the same time inhibiting the process by which the anomalous peaks are formed.

4.3 The Voltage Divider

Multiplication of the electrons in the PM tube occurs because the potential of each dynode is aranged so that it attracts the electrons ejected from the dynode preceding it. The resistance network that accomplishes this distribution of potentials is called the voltage divider, and adjustment of the resistors so as to achieve optimum PM performance is sometimes termed "tuning the PM tube".

If the PM power supply does not incorporate an internal voltage regulator the mains supply to it should be regulated. The anode pulse shape depends strongly on the applied voltage. Some PM tubes can be purchased ready-wired from the manufacturers. Recommended wiring diagrams can be obtained for all others. The wiring diagram is designed to divide the voltage

so as to ensure linear performance by preventing space charge saturation and by providing an average current far in excess (10–100 times) of that formed by the anode. If these criteria are fulfilled the voltage divider will in most cases be suitable for the SPC experiment. However, it is usually found that the performance of the PM, as regards the FWHM and secondary peaks of the instrument response function as well as the signal-to-dark count ratio, can be improved by slight departures from the manufacturer's recommendations. As a consequence, in SPC instruments the PM is generally wired with a number of variable resistors, which can be "tuned" to give the best overall operation.

A suitable voltage divider is most conveniently chosen by following one of the manufacturer's designs and allowing at least three (and perhaps more) resistors to be variable. These should be, in standard end-on tubes, between the cathode (K) and grid (G), grid and first dynode (D_1), and last dynode and earth. Possible voltage divider designs for the popular 56 DUVP and XP2020 PM tubes are illustrated in Fig. 4.5 and 4.6, respectively. In the former there is provision for seven variable resistors, but it is usually found that all reasonable values of R_3–R_6 do not affect the measured instrument response function. Since variable resistors are relatively bulky it is preferable to employ only as many of them as can be accommodated in a compact r.f.-tight housing. Long leads from the PM pins to a separate box holding the voltage divider may function as antennae and should be avoided. Fixed resistors are of the precision carbon film variety since wirewounds have a high inductance and are not suitable. Capacitors, of the ceramic disc (low inductance) variety, are connected in parallel with the resistors over the last few stages in order to prevent space charge saturation at the pulse peaks. Moulded track miniature potentiometers with insulated spindles are satisfactory as variable resistors. If they are wired as rheostats, as illustrated in Fig. 4.5 and 4.6, the resistance (but not the potential) between separate stages can be altered more or less independently. It should be remembered that the potentiometer casings are not at earth potential and should therefore be mounted on an insulating platform, as illustrated in Fig. 4.4 (A diagram of a voltage divider suitable for a 9 stage side-on PM tube can be found in the recent publication of Ware *et al.* (1983)).

Direct wiring of the photomultiplier pins to the voltage divider mounted on a circuit board is reported to improve the noise counts (Lytle, 1974) but it is more usual to make use of the base with mounting sockets supplied by the manufacturer. Cable lengths should be as short as possible and solder joints clean and true. It is usual to use a 50 Ω load resistor from the anode to earth in order to attain a fast rise time in the associated electronics (Lytle, 1974) but we have found that any value for this resistor up to 10 kΩ leads to similar performance. In fact the 50 Ω input impedance of the following amplifier or discriminator can serve as the load resistor for the anode, but if no bleed

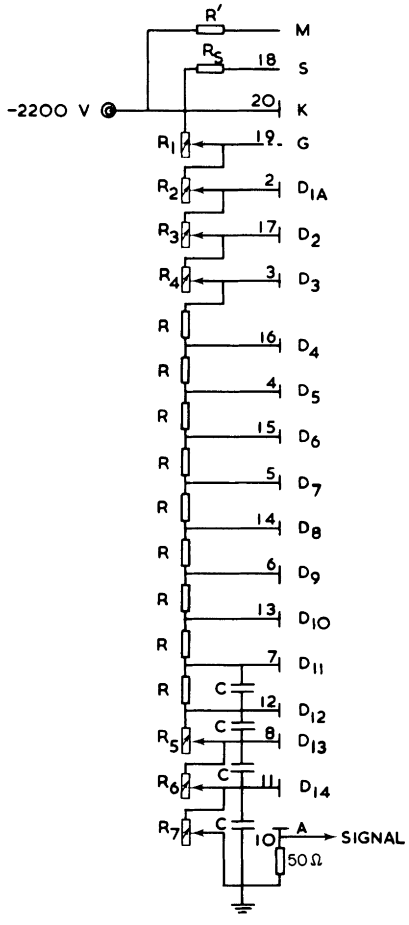

Figure 4.5 Suggested design of voltage divider for 14-stage Philips 56 DUVP photomultiplier. M, mu-metal screen; S, aquedag shield (internal connection); K, photocathode; G, grid (focussing electrode); D_{1A}, accelerating electrode and dynode 1; D_2–D_{14}, dynodes; A, anode; R_S, internal resistance (*c.* 16 MΩ); R_1–R_7, variable resistors (rheostats); R′,R, fixed resistors; C, capacitors. Suggested values: R′, 6 MΩ; R_1(0–20 kΩ), 6 kΩ; R_2(0–200 kΩ), 100 kΩ; R_3(0–60 kΩ), 40 kΩ; R_4(0–150 kΩ), 80 kΩ; R, 40 kΩ; R_5(0–100 kΩ), 40 kΩ; R_6(0–100 kΩ), 40 kΩ; R_7(0–100 kΩ), 40 kΩ; C, 10 nF.

resistor is employed great care must be taken to avoid damage to the electronics caused by the build up and sudden discharge of a high charge on the anode. Fifty ohm coaxial cable should be attached directly to the anode pin and earth connections made to a common earth. In order to seal the PM from r.f. interference all apertures should be as small as possible and the bulkhead connectors on the back plate should be of the type that can be

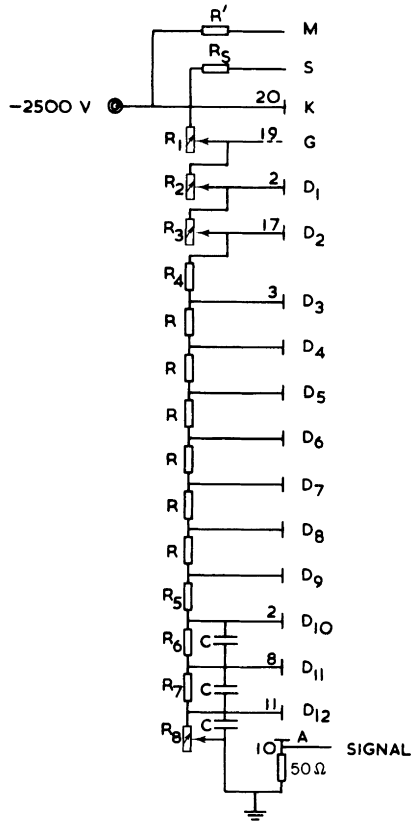

Figure 4.6 Suggested voltage divider design for 12-stage Philips XP2020 photomultiplier. M, mu-metal screen; S, aquedag shield (internal connection); K, photocathode; G, grid; D_1–D_{12}, dynodes; A, anode; C, capacitors; R_S, internal resistance; R′, R, R_4–R_7, fixed resistors; R_1–R_3, R_8, variable resistors (rheostats). Suggested values: R′, 6 MΩ; R_1(0–2 MΩ), 1.19 MΩ; R_2(0–2 MΩ), 940 kΩ; R_3(0–2 MΩ), 222 kΩ; R_4, 470 kΩ; R, 270 kΩ; R_5,R_6, 370 kΩ; R_7, 470 kΩ; R_8(0–2 MΩ), 600 kΩ; C, 10 nF.

sealed with a solder gasket (see Section 3.3.6). As an added precaution the potentiometer spindles can be taken out of the housing through waveguides attached to the back plate and sealed with solder gaskets.

Dark current may be reduced, as was stated in Section 4.2.3, if the pins are connected so that the cathode is at earth potential (Halpern, 1974; Leskovar *et al.*, 1976). This type of wiring is not common since it is necessary to couple the anode capacitively to the rest of the apparatus through an appropriately rated blocking capacitor. A positive high voltage is then applied to the last dynode. In addition to the hazard associated with degradation of the blocking capacitor there is also a risk, when the PM power supply voltage is

adjusted, of inducing fast transient voltages of sufficient amplitude to damage electronic components. Nevertheless it is in theory reasonable to maintain the tube envelope at the same potential as the surrounding housing.

With reference to Fig. 4.6 a suggested procedure for choosing resistor values and tuning the divider can be outlined. The data sheet for the XP2020 PM tube gives the maximum current formed by the anode as 0.2 mA. This is the maximum current capable of being generated by the cascade of electrons from dynode to dynode. In single photon counting detection the light levels are so low that this figure can be reduced by some orders of magnitude, say, to 10^{-6} A. As was stated previously the current along the chain should be about 100 times greater (10^{-4} A minimum), setting a maximum value for the total chain resistance, at an applied potential of 2.5×10^3 V, at 25 MΩ, well above the 6.25 MΩ of the chain in Fig. 4.6. If the current is too high the power dissipation ($V \times I$) may generate too much heat. Consequently the resistors are kept fairly large. Since the current in the chain is $(2.5 \times 10^3/6.25 \times 10^6)$ A $= 0.4$ mA, the power dissipated in the stage with the maximum voltage drop (K–G) is $I^2R = 0.19$ W. Therefore resistors rated at 0.25 W are satisfactory and are, moreover, conveniently small.

On the data sheet for the PM are also specified upper limits to the potentials to be applied between the various dynodes. While these recommendations are probably somewhat conservative it is found that too large a voltage drop between K and D_1 tends to induce a higher dark current. A large voltage drop, however, usually decreases the transit time spread. Hence a potential difference close to that specified as an upper limit by the manufacturer is probably a good compromise. For the XP2020 PM tube the recommendation is 800 V and the voltage divider suggested in Fig. 4.6 would provide 806 V at an applied voltage of 2500 V.

When the base has been wired and the resistances checked, pointers can be attached to the projecting spindles, and dials written on to the outside of the back plate so that the resistance produced by an adjustment of the spindle can be read off. In a rigorous adjustment procedure each resistance change should be accompanied by a change either in the applied high voltage or in the discriminator level in the CFTD. However, a purely empirical procedure in which only the PM resistors are altered will probably suffice.

The PM high voltage, which should be close to the highest value recommended by the manufacturers, is chosen together with a fairly low CFTD level, say 30–40 mV. An instrument response function is then collected, after the variable resistors have been set so as to achieve maximum counts. A note is then made of count rate, dark rate, and the shape of the instrument response function, particularly its FWHM and the intensities in any secondary peaks. Each rheostat is now adjusted in turn, but within a range in which the signal-to-dark count ratio is close to its highest value, and

a note made of the shape of the instrument response function for each adjustment. It will probably be noticed that the most satisfactory shape is obtained with resistor settings that also yield close to the highest count rate, although some decrease from the maximum is to be expected. A secondary peak preceding the main peak in the instrument response function should be eliminated entirely, but it will probably be necessary to strike a compromise between minimum FWHM and minimum intensity in the secondary following the main peak. If the latter can be eliminated without a significant increase in the FWHM, so much the better. When the settings that yield the best compromise between high count rate, low dark current, narrow FWHM and minimum intensity in secondary peaks have been determined, a calculation is made to ensure that the resistances chosen do not give an excessive potential drop between any two stages. Finally the decay curve of a standard sample is collected and deconvolved. If the result is not satisfactory, and other sources of error can be ruled out, the resistors are re-tuned so that the compromise is biased in a different direction and deconvolution repeated. Once satisfactory settings have been attained re-tuning should not be necessary for a matter of months or even years.

The foregoing procedure refers primarily to end-on type PM tubes. Our experience with side-on types indicates that constant interdynode voltage all along the chain with capacitors in parallel with resistors across the last few stages leads to the best results.

4.4 Wavelength Dependence of Transit Time

The energy of the electron ejected from the photocathode depends on the work function of the cathode material and the energy of the incident photon. It has in the past been observed that, in spite of the developments in electrostatic focussing designed to minimize the effect of velocity variations in primary photoelectrons on the transit time through the dynode chain, the shape of the observed instrument response function depended on the wavelength at which it was measured (Lewis *et al.*, 1973; Wahl *et al.*, 1974; Andre *et al.*, 1979; Peterson *et al.*, 1979). In fact fast PM tubes are reported to show up to a four-fold increase in dispersion when the wavelength of the incident photons is reduced from 600 nm to 300 nm (Pietri and Nussli, 1968), with the main difference occurring in the cathode to first dynode region (Moszynski and Vacher, 1977). At the same time the actual transit time is expected to decrease in accordance with Equation 4.3. There have also been reports that some PM tubes with red-sensitive photocathodes such as the Philips XP1023 (Grinvald, 1976), the RCAC31034 (Spears *et al.*, 1978) and the Hamamatsu R928 (Ware *et al.*, 1983) show few wavelength effects.

A number of attempts have been made to ascertain to what extent observed wavelength variations in instrument response functions arise from PM effects. The difficulty arises because when the instrument response function is measured at different wavelengths observed variations may also result from pump pulse wavelength variations. In order to resolve this difficulty Ware and co-workers (Lewis *et al.*, 1974) measured instrument response functions at different wavelengths, both with and without a quantum counter placed in front of the photomultiplier. Light in the wavelength range of interest is totally absorbed by the quantum counter, the emission characteristics of which are assumed not to vary with excitation wavelength. Therefore the PM is exposed to photons of the same energy irrespective of the wavelength of the lamp's radiation. The broadening due to the time response (fluorescence lifetime) of the quantum counter can be incorporated in the photomultiplier response function. That is, the observed function, $P'(\lambda_e,t)$, is given by:

$$P'(\lambda_E,t) = E(\lambda_E,t) \otimes G(\lambda_Q,t) \otimes H(\lambda_Q,t) \tag{4.5}$$

$$= E(\lambda_E,t) \otimes H'(\lambda_Q,t) \tag{4.6}$$

where $G(\lambda,t)$ is the decay function of the quantum counter, λ_Q is the wavelength of quantum counter fluorescence, and the other symbols are as explained in Section 2.3. Of course the lifetime of quantum counter fluorescence should be as short as possible so that changes in $P'(\lambda_e,t)$ are not obscured by the extra convolution. It will now be understood that if $P(\lambda_E,t)$, given previously by Equation 2.20 as:

$$P(\lambda_E,t) = E(\lambda_E,t) \otimes H(\lambda_E,t)$$

shows a variation with λ_E that is not present in the function $P'(\lambda_E,t)$, the variation is a result of PM effects. The authors were able to conclude that both lamp and PM contributed to the overall effect but that the PM was mainly responsible. [Insertion of the quantum counter, sometimes called a wavelength shifter, in *all* SPC measurements could also serve to correct for the wavelength effects (Upton and Cline Love, 1979; Peterson *et al.*, 1979). It is not recommended because it reduces the sensitivity of the instrument and depends too critically upon the invariance of quantum counter fluorescence decay function on excitation wavelength.]

A further investigation of this problem, with wavelength independent pulses from a storage ring source, was carried out, again by Ware and co-workers (Andre *et al.*, 1979). In this experiment wavelength variations in the instrument response function must arise from PM effects. Since the shape of the storage ring pulse can be calculated the response functions of the PM tube can be derived. This function, for the EMR 651F-09-13 PMT, is shown

at two wavelengths in Fig. 4.7. While the difference in FWHM between the two functions is not significant (FWHM is expected to, and is usually observed to, increase at shorter wavelength) the change in shape at longer times is quite marked.

On nanosecond timescales the pulses that are derived from synchronously pumped dye lasers (see Section 3.4.4) can be regarded as δ-functions since their FWHM is less than 10 ps. Consequently changes in shape within the time scale of 10 ps, as for instance upon second harmonic generation, will have only a minimal effect on instrument response functions measured on a nanosecond timescale. The change in the instrument response function between measurements at the doubled and undoubled light wavelengths should therefore be, to all intents and purposes, the change in the PM response function between these two wavelengths. These changes are illustrated by the functions shown in Figs 4.8, 4.9 and 4.10. In Fig. 4.8 are shown instrument response functions collected at 600 nm and 300 nm for an XP2020Q photomultiplier with two different voltage dividers. Clearly, the function shifts with wavelength. In addition in (b) a gross shape change is evident, whereas in (a) the change is not so obvious. In Fig. 4.9 the curves in Fig. 4.8(b) have been drawn with peak positions coincident in order to compare more closely the shape of the functions. Apart from some broadening in the wings at 600 nm the curves are not very different. It is worthy of note that the 600 nm function in Fig. 4.8(a) is considerably narrower than the

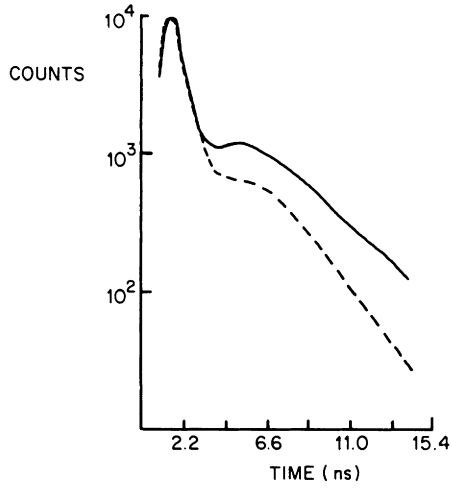

Figure 4.7 Response function of EMR 561F-09-13 photomultiplier at 220 nm (——) and 170 nm (- - - - -). Reported FWHM at 220 nm was 1.31 ns and at 170 nm 1.21 ns (after Andre *et al.*, 1979).

600 nm function in (b), indicating that, when tuning the voltage divider, the FWHM of the instrument response function should not be the only guide. As a matter of fact both of the u.v. functions in Fig. 4.8 could be deconvolved quite satisfactorily from decay curves so that from this point of view it would be misleading to state that the voltage divider for (a) was maladjusted. Nevertheless, we feel that the PM tuning that produces the least shape change with wavelength is to be preferred.

Instrumental methods of correcting for PM wavelength effects are discussed in Section 2.3 and mathematical corrections in Section 6.3. Among the latter, the most common rests on the assumption that a wavelength-dependent PM response results merely in a time shift in the measured curve. In effect it is assumed that the photoelectron transit time varies but that the transit time spread remains constant. This assumption is perhaps a simplification but finds some support in the curves illustrated in Fig. 4.8(a) and 4.9. The shift to be seen in Fig. 4.8(a) is illustrated more clearly by the log plots in Fig. 4.10. Here there is again a slight change of shape but the major difference between the functions, again measured at 300 nm and 600 nm, is the shift along the time axis. The displacement is about 400 ps, in fair agreement with the figure of 1 ps per nm reported for this PM tube by Robbins *et al.* (1980). In Table 6.1 we show that mathematically a shift is an adequate correction for the wavelength effect. That it is may be explained by the mode of signal processing employed in the SPC measurement. Although the PM anode

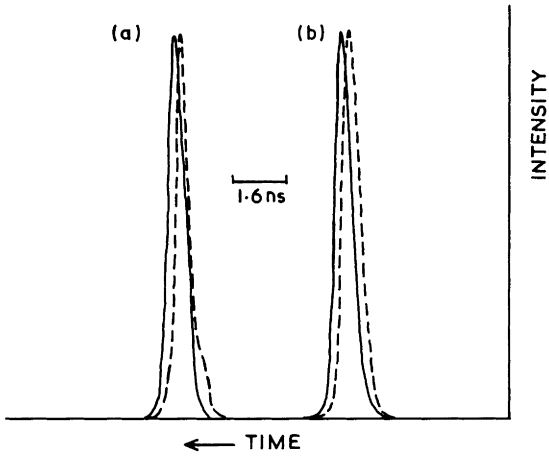

Figure 4.8 Instrument response functions of the fundamental, 600 nm (- - - -) and frequency-doubled, 300 nm (——) output of a synchronously pumped dye laser. The laser pulses, extracted with a cavity-dumper, have an FWHM of *c.* 6 ps. (a) and (b) represent the results of measurements with slightly different PM voltage divider.

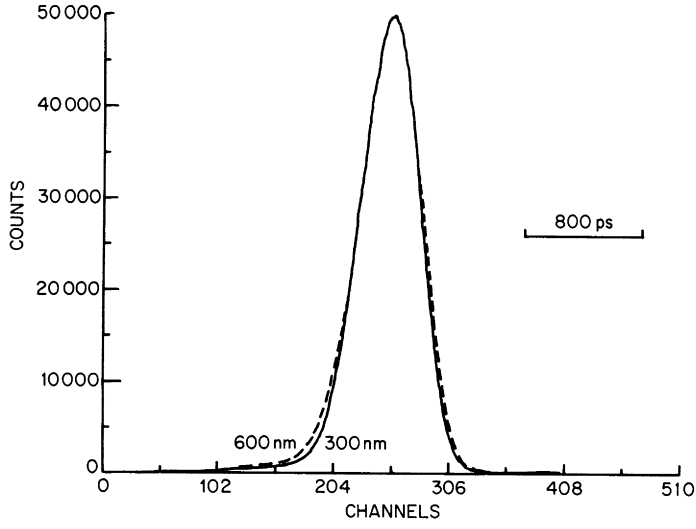

Figure 4.9 Comparison of the shape change of an instrument response function measured at 600 nm and 300 nm. Conditions are as in Fig. 4.8(b).

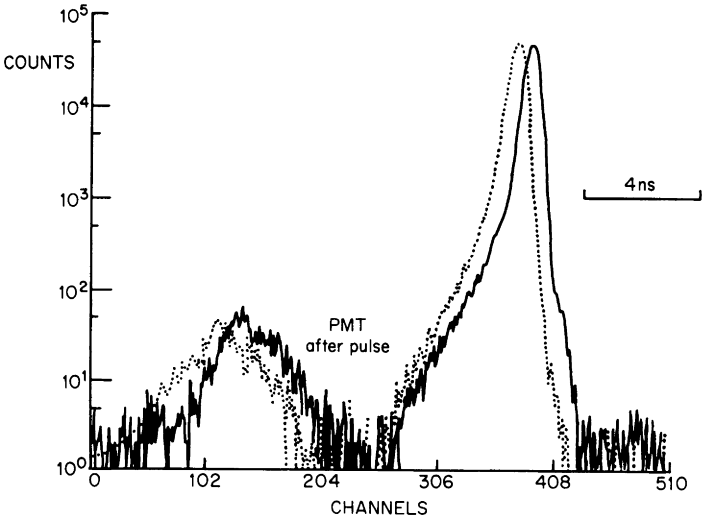

Figure 4.10 Comparison on a vertical log scale and expanded horizontal scale of functions measured under identical conditions as those in Fig. 4.8(b) (- - - - -) 600 nm (——) 300 nm. Inverted TAC configuration.

pulse shape may vary with wavelength, the discriminator, which times from some point on the leading edge of the pulse, sees the variation merely as a time shift. In the light of the increased dispersion in fast PM tubes at shorter wavelengths this explanation seems somewhat simplistic. Nevertheless, the shift correction appears to be satisfactory in the analysis of nanosecond decays; whether it will remain so for picosecond decays remains to be seen. There is some evidence however that modern developments in PM technology are reducing these potentially serious wavelength affects. Ancillary difficulties associated with a mathematical shift routine are discussed in Chapter 6.

4.5 New Developments

With the increasing proliferation of picosecond lasers as excitation sources in single photon counting instruments the demand for PM tubes with transit time spreads, and therefore δ-function responses, in the tens rather than hundreds of picoseconds has risen. The most promising development has been the microchannel plate PM tube. It was also hoped to improve timing characteristics by replacing the purely electrostatic electron focussing of conventional PM tubes by focussing achieved with crossed electric and magnetic fields.

The performance of a static crossed-field PM, the Varian VPM-154, has been described by Koester (1979). Since the excitation source in his instrument was a picosecond laser, the duration of the pump pulse made a negligible contribution to the width of the instrument response function. The crossed-field PM has a low gain and must be coupled to an amplifier. Although the transit time dispersion was reported to be less than 30 ps the instrument response function had a FWHM of 228 ps, compared with 760 ps for an RCA 31034 and 360 ps for the RCA 8850. It is likely that the amplifier made a large contribution to this FWHM so that the improvement in PM performance is quite significant. Nevertheless instrument response functions of similar FWHM have been obtained with much less expensive PM tubes (Robbins *et al.*, 1980).

More promising than the crossed-field PM is the microchannel plate PM (Barker and Weston Jr., 1976; Yamazaki *et al.*, 1982). A microchannel plate is a secondary electron multiplier consisting of an array of millions of glass capillaries (called channels) with internal diameters 10 μm to 20 μm. These capillaries are fused into the form of a thin (< 1 mm) disc and the inside walls are coated with a secondary electron emissive material. Both ends of the channels are covered with a thin metal film which acts as the electrode. A schematic representation of electron amplification in a single channel is given

in Fig. 4.11(a) and of a microchannel plate PM tube in Fig. 4.11(b). It can be seen that the channels are sliced at an angle in order to prevent passage of the primary electron through the channel without striking the wall.

Among the drawbacks associated with microchannel plate PM tubes are ion feedback causing reduced photocathode lifetime and after-pulsing, and reduced counting rate resulting from the "dead time" required to neutralize the residual positive charge remaining in the channel after passage of the electron current. It is also reported that data distortions introduced by this type of PM are progagated differently in instrument response function and decay curve, i.e., that successful data deconvolution is difficult to achieve (Fleming, 1983). On the other hand these PM tubes are extremely fast with a very small transit time spread, have good single photon resolution and can achieve relatively high gains through incorporation of two or three microchannel plates. In addition they are reported to be subject to very small or negligible wavelength effects (Yamazaki, 1982). Dark current in microchannel PM tubes with red-sensitive photocathodes can be quite high, however; there appears to be no cooled housing available commercially at the time of writing.

In Fig. 4.12 is illustrated the instrument response function obtained for a picosecond pulse from a synchronously pumped dye laser with a Hamamatsu

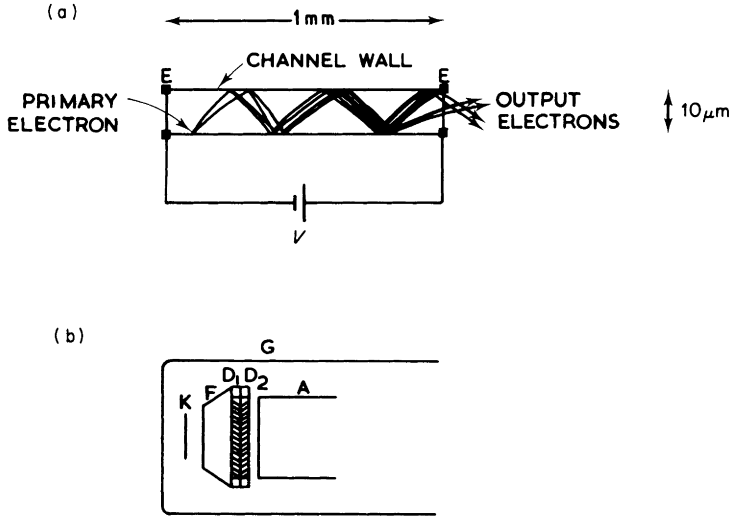

Figure 4.11 Schematic representation of (a) electron amplification in a single microchannel. E, electrodes. Parabolic trajectories determined by initial velocity. (b) PM tube with two microchannel plate discs D_1 and D_2. G, glass envelope; F, focus; K, semi-transparent photocathode; A, anode.

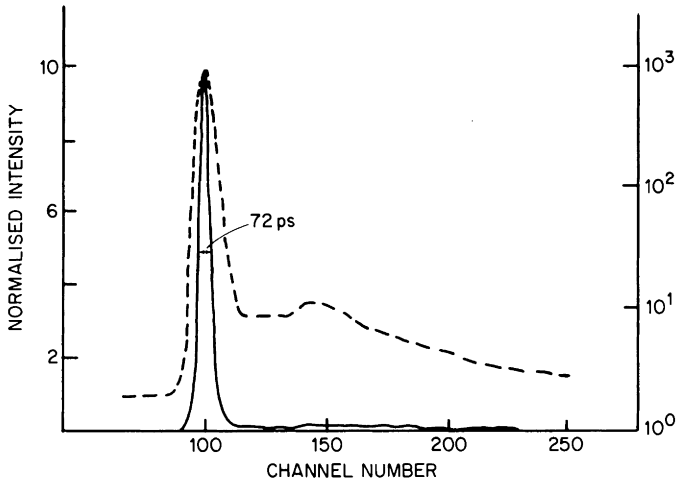

Figure 4.12 Instrument response function for laser pulse (FWHM 6 ps) obtained with Hamamatsu R1294U PM operated at 3000 V. (——) linear plot (- - - - -) log plot. 12.8 ps per channel. (Yamazaki, 1982).

R1294U two-stage microchannel plate PM tube operated at 3000 V. The FWHM of this function is 72 ps, considerably shorter than has been reported for conventional or crossed-field PM tubes. It should be noted, however, that electronic processing of the PM signals was carried out with the latest generations of electronic components, specifically a Hewlett Packard 8447D 1 GHz preamplifier, Ortec 583 CFTD incorporating an upper level discriminator (allowing selection of single photon pulses), and Ortec 467 TAC. Because signal transmission from PM tube to amplifier and discriminator can contribute substantially to the width of measured instrument response functions (Robbins *et al.*, 1980) the extremely narrow function in Fig. 4.12 is a result partly of decreased electronic jitter. Nevertheless, the performance of the PM is quite impressive. Recently Hamamatsu have produced a new "proximity type" two-stage microchannel PM tube, which is reported to yield an even narrower δ-pulse response function (Yamazaki, 1982). It will be noted that this PM produces a long tail, probably owing to ion feedback effects. It is to be hoped that in the development of these PM tubes, at present at a relatively early stage, this problem can be eliminated. At the time of writing the two-stage Hamamatsu microchannel PM tube costs about twice as much as conventional 12- or 14-stage end-on type PMs. It is possible that the cost will be reduced once production increases but even at the present price this type of PM must be seriously considered by the SPC user who intends to measure ps lifetimes. Further details can be found in Appendix 4.A1.

References

Andre, J. C., Lopez-Delgado, R., Lyke, R. L. and Ware, W. R. (1979). *Appl. Optics* **18**, 1355–1359.

Barker, J. R. and Weston Jr., R. E. (1976). *J. Chem. Phys.* **65**, 1427–1442.

Beck, G. (1976). *Rev. Sci. Instrum.* **47**, 537–541.

Birks, J. B. and Munro, I. H. (1967). *Prog. React. Kinet.* **4**, 239–303.

Coates, P. B. (1975). *J. Phys. E.* **8**, 614–617.

Coates, P. B. and Andrews, J. W. (1981). *J. Phys. E.* **14**, 1164–1166.

Fenster, A., LeBlanc, J. C., Taylor, W. B. and Johns, H. E. (1973). *Rev. Sci. Instrum.* **44**, 689–694.

Fleming, G. R. (1983). Private communication.

Foord, R., Jones, R., Oliver, C. J. and Pike, E. R. (1969). *Appl. Optics* **8**, 1975–1989.

Grinvald, A. (1976). *Anal. Biochem.* **75**, 260–280.

Gulari, E. and Chu, B. (1977). *Rev. Sci. Instrum.* **48**, 1560–1567.

Halpern, A. M. (1974). *J. Amer. Chem. Soc.* **96**, 7655–7661.

Hartig, P. R., Sauer, K., Lo, C. C. and Leskovar, B. (1976). *Rev. Sci Instrum.* **47**, 1122–1129.

Jones, R., Oliver, C. J. and Pike, E. R. (1971). *Appl. Optics* **10**, 1673–1680.

Kinoshita, S., Ohta, H. and Kushida, T. (1981). *Rev. Sci. Instrum.* **52**, 572–575.

Koester, V. J. (1979). *Anal. Chem.* **51**, 458–459.

Kouyama, T. (1978). *Jpn. J. Appl. Phys.* **17**, 1409–1418.

Lampert, R. A. (1981). Personal communication.

Lampert, R. A., Chewter, L. A., Phillips, D., O'Connor, D. V., Roberts, A. J. and Meech, S. R. (1983). *Anal. Chem.* **55**, 68–72.

Leskovar, B., Lo, C. C., Hartig, P. R. and Sauer, K. (1976). *Rev. Sci. Instrum.* **47**, 1113–1121.

Lewis, C., Ware, W. R., Doemeny, L. J. and Nemzek, T. L. (1973). *Rev. Sci. Instrum.* **44**, 107–114.

Longworth, J. W. (1977). *Photochem. Photobiol.* **26**, 665–668.

Lopez, R. J. and Rebolledo, M. A. (1981). *Rev. Sci. Instrum.* **52**, 1852–1854.

Lyke, R. L. and Ware, W. R. (1977). *Rev. Sci. Instrum.* **48**, 320–326.

Lytle, F. E. (1974). *Anal. Chem.* **46**, 545A-557A.

Morton, G. A. (1968). *Appl. Optics* **7**, 1–10.

Morton, G. A., Smith, H. M. and Krall, H. R. (1968). *Appl. Phys. Lett.* **13**, 356–357.

Moszynski, M. and Vacher, J. (1977). *Nucl. Instrum. Meth.* **141**, 319–323.

Petersen, S. H., Demas, J. N., Kennelly, T., Gafney, H. and Novak, D. P. (1979). *J. Phys. Chem.* **83**, 2991–2996.

Pietri, G. and Nussli, J. (1968). *Philips Tech. Rev.* **29**, 267–287.

Poultney, S. K. (1972). *Adv. Elect. Elect. Phys.* **31**, 39–117.

Robbins, R. J., Fleming, G. R., Beddard, G. S., Robinson, G. W., Thistlethwaite, P. J. and Wolfe, G. J. (1980). *J. Amer. Chem. Soc.* **102**, 6271–6279.

Samson, J. A. R. (1967). "Techniques of Vacuum Ultra-violet Spectroscopy", pp. 188–205. John Wiley, New York.

Schuyler, R. and Isenberg, I. (1971). *Rev. Sci. Instrum.* **42**, 813–817.

Spears, K. G. and Hoffland, L. D. (1977). *J. Chem. Phys.* **66**, 1755–1758.

Spears, K. G., Cramer, L. E. and Hoffland, L. D. (1978). *Rev. Sci. Instrum.* **49**, 255–262.

Stevens, S. S. and Longworth, J. W. (1972). *IEEE Trans. Nucl. Sci.* **NS-19**, 356–359.

Swords, M. D. (1977). Thesis. University of Southampton.

Timothy, J. G. and Bybee, R. L. (1977). *Rev. Sci. Instrum.* **48**, 292–299.

Upton, L. M. and Cline Love, L. J. (1979). *Anal. Chem.* **51**, 1941–1945.
Wahl, Ph., Auchet, J. C. and Donzel, B. (1974). *Rev. Sci. Instrum.* **45**, 28–32.
Ware, W. R., Pratinidhi, M. and Bauer, R. K. (1983). *Rev. Sci. Instrum.* **54**, 1148–1156.
Wright, A. G. (1981). *J. Phys. E* **14**, 851–855.
Yamazaki, I. (1982). Personal communication.
Yamazaki, I., Murao, T. and Yoshihara, K. (1982). *Chem. Phys. Lett.* **87**, 384–388.
Zimmerman, H. E., Werthmann, D. P. and Kamm, K. S. (1974). *J. Amer. Chem. Soc.* **96**, 439–449.

Appendix 4.A1

In Table 4.A1 we give details of PM tubes that appear to have been most commonly used in SPC measurements. Also listed are some less popular tubes that appear to have some unique advantages. We need hardly stress that the list is by no means exhaustive. Nor is it meant to be assumed that we believe PM tubes in this list are more suitable for SPC instruments than others that we do not refer to.

The figures for cost are approximate and are given in pounds (£) sterling.

Users of all the tubes listed have already been referred to in this chapter unless indicated by a superscript.

Figures for gain, transit time and anode pulse rise time have been taken, for the most part, from the manufacturers' literature. As regards transit time and anode pulse rise time the figures are not of great use since it is generally true that the manufacturers specifications can be improved considerably by voltage divider tuning. In addition the gain can be increased by operating the PM at a higher voltage than that applied in the manufacturers' tests.

Appendix 4.A2

The following companies manufacture photomultiplier tubes that are suitable for single photon counting and timing. In addition to their normal catalogues some manufacturers publish applications manuals containing a wealth of theoretical and practical information. Some of these publications are given with the address of the corresponding manufacturer.

(1) Philips, Eindhoven, The Netherlands.
[Amperex Fast Response Photomultipliers.]

(2) RCA, Harrison, New Jersey, USA.
[RCA Photomultiplier Manual.]

(3) Thorn/EMI, Hayes, Middlesex, UK.
[EMI Photomultiplier Manual and Application Notes.]

(4) Hamamatsu TV Company Limited,
1126 Ichino-cho, Hamamatsu, Japan.

(5) Varian Instrument Division,
611 Hansen Way, Palo Alto, California 94303, USA.

(6) ITT Electronic Services,

(7) EMR Photoelectric, P.O. Box 44, Princeton, New Jersey 08540, USA.

For PM Housings

(8) Products for Research Incorporated
78 Holton Street, Danvers, Massachusetts 01923, USA.

Table 4.A1

Manufacturer and Model No.	Spectral response (cathode material)	Gain (at applied voltage)	Anode pulse rise time/ns	Transit time/ns	Remarks	Cost £ sterling
EMI 9594QB[a]	200–750 nm S-20 ($CsNa_2KSb$)	1×10^7 (2900 V)	2	50	14 stages. Equivalent of 56DUVP	[h]
EMI 9863 QB	S-20	2.5×10^7 (2600 V)	2.5	45	Red sensitive. 1 cm diameter cathode[b]	997
Philips 56DUVP/03	200–600 nm (KCsSb)	2×10^8 (2200 V)	2	43	14 stages specially selected for low dark counts	[i]
Philips XP2020Q	200–600 nm (KCsSb)	3×10^7 (2200 V)	1.5	28	12 stages	450
RCA 8850	200–600 nm (KCsSb)	7×10^6 (2000 V)	2.1	31	12 stages. Good single photon resolution	640
RCA 8575[c]	200–600 nm (KCsSb)	1×10^7 (2000 V)	2.5	30	As for 8850	297
RCA C31034	200–950 nm (GaAs)	6×10^5 (1500 V)	2.5[d]	30	11 stages. Good SP resolution very flat response	827

RCA 1P28	250–600 nm (S-5)	2.5×10^6 (1000 V)	1.6	20	Side-on inexpensive	41
Hamamatsu R928	200–930 nm (NaKCsSb)	2×10^7[e] (1000 V)	2.2	22	As for 1P28 but red sensitive	112
EMR 561F-09-13	120–320 nm (CsTe)	1×10^7[f] (3000 V)	*c.* 2	*c.* 20	Solar blind. 13 stages. MgF_2 window, very low dark count	[j]
Varian VPM 154A-6D	200–1100 nm (InGaAsP)	1×10^5 (3300 V)	0.12	~1	Crossed field. Very expensive	>5000
Hamamatsu R1294 U-01	300–850 nm (NaKCsSb)	1×10^7 (3000 V)	[g]	~1	Microchannel plate	2500

[a]Reference: Swords, 1977.
[b]Small photocathode area reduces sensitivity but increases time resolution.
[c]Reference: Zimmerman *et al.*, 1974.
[d]Given as 0.8 ns by Lytle, 1974.
[e]This value from Kinoshita *et al.*, 1981.
[f]This value from Lyke and Ware, 1977.
[g]See Section 4.5.
[h]No longer available. Nominal replacement is EMI 9813QB at £391.
[i]No longer available. Nominal replacement is XP2020.
[j]Must be ordered.